^{57}Fe Mössbauer spectral and muon spin relaxation study of the magnetodynamics of monodispersed γ-Fe_2O_3 nanoparticles

Leïla Rebbouh, Raphaël P. Hermann,* and Fernande Grandjean†
Department of Physics, University of Liège, B5, B-4000 Sart-Tilman, Belgium

Taeghwan Hyeon‡ and Kwangjin An
National Creative Research Initiative Center for Oxide Nanocrystalline Materials and the School of Chemical and Biological Engineering, Seoul National University, Seoul 151-744, Korea

Alex Amato§
Laboratory for Muon Spin Spectroscopy, Paul Scherrer Institut, CH-5232 Villigen, Switzerland

Gary J. Long‖
Department of Chemistry, University of Missouri–Rolla, Rolla, Missouri 65409-0010, USA
(Received 4 May 2007; revised manuscript received 17 July 2007; published 13 November 2007)

The Mössbauer spectra of monodispersed iron oxide nanoparticles with diameters of 4, 7, 9, and 11 nm have been measured between 4.2 and 315 K and fitted within the formalism for stochastic fluctuations of the hyperfine Hamiltonian. In this model, the hyperfine field is assumed to relax between the six $\pm x$, $\pm y$, and $\pm z$ directions in space with a distribution of relaxation rates that is temperature dependent. Muon spin relaxation measurements have been carried out on the 9 nm particles between 4.2 and 295 K. Both techniques reveal three regimes in the magnetic dynamics of these nanoparticles. In the low-temperature regime, between 4.2 and ~30 K, the nanoparticle magnetic moments are blocked and a spin-glass-like state is observed with nearly static hyperfine fields, as is indicated by the well resolved magnetic Mössbauer spectra and the slow exponential decay of the muon asymmetry functions. In the high-temperature regime, above ~125 K, the nanoparticle magnetic moments and, hence, the hyperfine fields, relax rapidly and a typical thermally activated superparamagnetic behavior is observed, as is indicated by the Mössbauer doublet line shape and the muon asymmetry functions that are unquestionably characteristic of monodispersed nanoparticles. In the intermediate regime between ~30 and 125 K, the Mössbauer spectra are the superposition of broad sextets and doublets and the muon asymmetry functions have been fitted with a sum of two terms, one relaxing term similar to that observed at and above 125 K and one term characteristic of static local fields. Hence, in this intermediate regime, the sample is magnetically inhomogeneous and composed of nanoparticles rapidly and slowly relaxing as a result of interparticle interactions. The magnetic anisotropy constants determined from both the Mössbauer spectral and magnetic susceptibility results decrease by a factor ~4 with increasing diameter from 4 to 22 nm and increase linearly with the percentage of iron(III) ions present at the surface of the nanoparticles. The interparticle interaction energy is estimated to be between 89 and 212 K from the temperature dependence of the magnetic hyperfine field measured on the 9 nm nanoparticles.

DOI: 10.1103/PhysRevB.76.174422 PACS number(s): 75.50.Tt, 76.75.+i, 76.80.+y

I. INTRODUCTION

Nanocomposite materials containing iron nanoparticles are highly interesting and have been extensively studied both because of their promising electrical, magnetic, and optical properties and because of their potential specific applications in photonics, catalysis, magnetic recording, and biological sensing.[1] The magnetic applications of iron oxide nanoparticles often place specific requirements on the particle size distribution, such as a narrow size distribution.[2] An excellent control of the crystallinity and the size distribution of iron oxide nanoparticles has recently been achieved[3] and the synthesis of monodispersed nanoparticles of a given diameter between 4 and 15 nm is now feasible. This synthesis has been achieved through the thermal decomposition of an iron-oleate complex which was prepared from the reaction of iron pentacarbonyl and oleic acid in octyl ether, followed by the controlled chemical oxidation using $(CH_3)_3NO$ as a mild oxidant. Transmission electron microscopy images have beautifully illustrated[4] the two-dimensional hexagonal assembly of these monodispersed particles. Zero-field and field cooled magnetic susceptibility measurements[3,5] on these monodispersed iron oxide nanoparticles have found blocking temperatures that increase from 8 to 275 K as their diameters increase from 4 to 15 nm.

Another technique of choice for the study of the magnetic behavior of iron containing nanoparticles is iron-57 Mössbauer spectroscopy. Over the past 20 years, this technique has been widely used[6–9] to characterize small iron oxide particles with both various size distributions and various intraparticle and interparticle interactions. The Mössbauer spectra of γ-Fe_2O_3 nanoparticles typically show rather sharp sextets at 4.2 K, a more or less broadened doublet at 295 K, and a superposition of very broad sextets and doublets at intermediate temperatures. Such spectra have usually been fitted[6,8] with distributions of hyperfine fields resulting from the par-

ticle diameter distributions; in many other cases the spectra simply have not been fitted.[7]

The complex magnetic behavior of γ-Fe_2O_3 nanoparticles between 4.2 and 295 K, as revealed by both the magnetic susceptibility and the Mössbauer spectral measurements, has led to the development of various models. The most substantiated model[7] suggests the existence of a spin-glass-like state at low temperatures and of a transition from this state to a superparamagnetic state at a higher critical temperature.

The interactions between magnetic nanoparticles have also been investigated[10–14] by magnetic and Mössbauer spectral measurements for a variety of nanoparticles with different sizes and compositions. Three regimes have been proposed; first, a collective dynamic regime for the particle magnetic moments at low temperatures; second, a purely superparamagnetic regime at high temperatures; and third, a superparamagnetic regime modified by the interparticle interactions at intermediate temperatures. The collective dynamic regime exhibits[13] similarities with a spin-glass regime. However, the precursor of the spin-glass regime is a paramagnetic state at high temperature, whereas the precursor of the collective dynamic regime is a superparamagnetic state, a state that is characterized by a distribution of relaxation times and blocking temperatures that may be associated with a distribution of particle sizes. Hence, a study of monodispersed iron oxide nanoparticles is essential to understand the exact nature of any low-temperature magnetic regime and the transition between the low- and high-temperature regimes.

Few experimental methods are able to distinguish between the paramagnetic to spin-glass transition and the superparamagnetic to spin-glass transition. To date ac susceptibility measurements have been used,[15] but the nonuniform size of the γ-Fe_2O_3 nanoparticles has led to broad peaks in the susceptibility, peaks that are similar to those observed in a spin-glass material. Thus ac susceptibility measurements often do not yield a definite conclusion concerning the low-temperature magnetic state of the γ-Fe_2O_3 nanoparticles. More recently, the application of μ-spin relaxation[16] to the study of magnetic nanoparticles has been proposed. Simulations have indicated that the relaxation functions associated with the three regimes; first, the collective or blocked or spin-glass-like regime; second, the intermediate regime; and third, the superparamagnetic regime, can be differentiated by μ-spin relaxation studies. Furthermore, these simulations have shown that the shape of the relaxation function is sensitive both to the width of the particle size distribution and to interparticle interactions.

Herein, the iron-57 Mössbauer spectral and μ-spin relaxation measurements on monodispersed iron oxide nanoparticles are presented and analyzed both as a function of temperature and particle size. The goals of this study are as follows: first, to better characterize the low-temperature magnetic regime of the nanoparticles; second, to investigate the promising sensitivity of the μ-spin relaxation measurements to the magnetodynamics of monodispersed nanoparticles; third, to study the sensitivity of the Mössbauer spectra to the monodispersed nature of the nanoparticles; and finally, to compare and contrast the nature of the magnetodynamics obtained from various different techniques.

II. EXPERIMENT

Monodispersed iron oxide nanoparticles with diameters of 4.0(1), 7.0(2), 9.0(2), and 11.0(2) nm have been prepared as previously described.[3–5] Earlier studies[5] have indicated that these particles have a diameter distribution with a standard deviation of less than 5%. One-half of this deviation is quoted above as the accuracy of the particle diameters. These particles are coated with oleic acid and transmission electron microscopy[4] indicates that there is an ~3 nm layer of oleic acid around the 9 nm particles. Hence, the distance between the centers of two particles is ~12 nm. Similar coatings of oleic acid exist around the other particles. Furthermore, these previous studies[5] have also indicated that in some cases the nanoparticles consist of $(\gamma\text{-}Fe_2O_3)_{1-x}(Fe_3O_4)_x$ solid solutions with x ranging from 0.2 to 0.5. However, the Mössbauer spectral results presented below do not support the presence of more than 5%–10% of Fe_3O_4 in the nanoparticles understudy herein.

The iron-57 Mössbauer spectra have been measured between 4.2 and 315 K on a constant acceleration spectrometer which utilized a rhodium matrix cobalt-57 source and was calibrated at 295 K with α-iron foil. The isomer shifts are reported relative to α-iron at 295 K. The absorber thicknesses were ~44 mg/cm^2 of sample.

The μ-spin relaxation measurements were carried out on the GPS instrument at the Paul Scherrer Institute, Villigen, Switzerland, with 16 keV spin-polarized muons. The measurements were carried out on the 9 nm iron oxide nanoparticles at an absorber thickness of 150 mg/cm^2 in a zero applied field between 5 and 300 K.

III. MÖSSBAUER SPECTRAL RESULTS

The Mössbauer spectra of the 4, 7, 9, and 11 nm diameter iron oxide nanoparticles obtained at 295, 85, and 4.2 K are shown in Figs. 1–3, respectively. At 295 K the spectra consist of a doublet with an additional broadened component, a component whose area decreases with decreasing diameter. At 4.2 K the spectral lines are rather narrow and exhibit fully developed sextets for all of the nanoparticle diameters. In contrast, as a comparison of Figs. 1–3 clearly indicates, the four 85 K spectra are somewhat different especially for the smallest diameter particles. More specifically, as the diameter decreases, the spectra change from rather well-defined sextets for the 11 nm particles to a spectrum that is dominated by a doublet for the 4 nm particles.

The temperature dependence of the Mössbauer spectra of the 4 and 9 nm iron oxide nanoparticles is shown in Figs. 4 and 5, respectively. Except for the temperature shift, the qualitative temperature dependence is similar for both the 4 and 9 nm particles. Starting from well-defined sextets at 4.2 K, the spectra sequentially change to broadened sextets, to a superposition of highly broadened sextets and doublets, and, finally, to a broadened doublet at the higher temperatures. As expected, the change to a doublet occurs at lower temperatures for the 4 nm iron oxide nanoparticles than for the 9 nm nanoparticles. Hence, the general behavior of the spectra is similar to that expected for a superparamagnetic

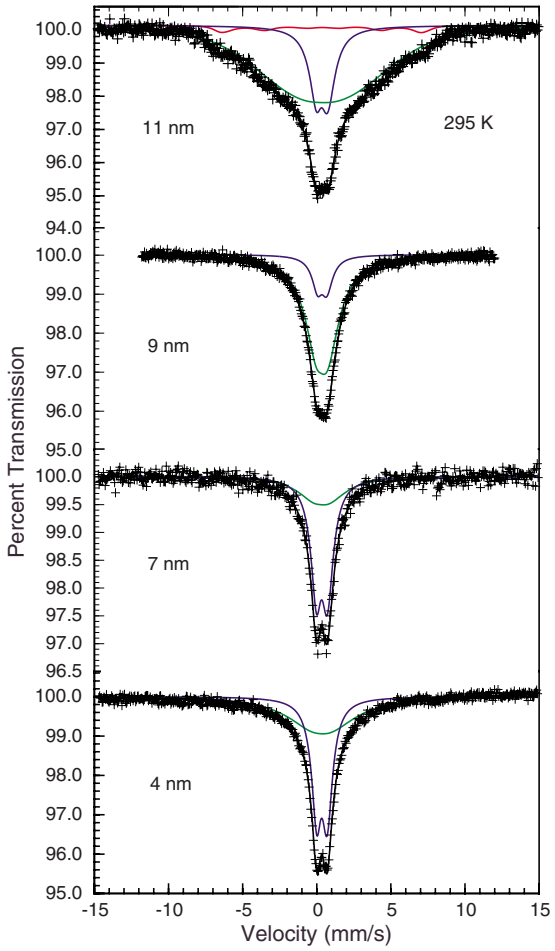

FIG. 1. (Color online) The 295 K Mössbauer spectra of the iron oxide nanoparticles with the indicated diameters.

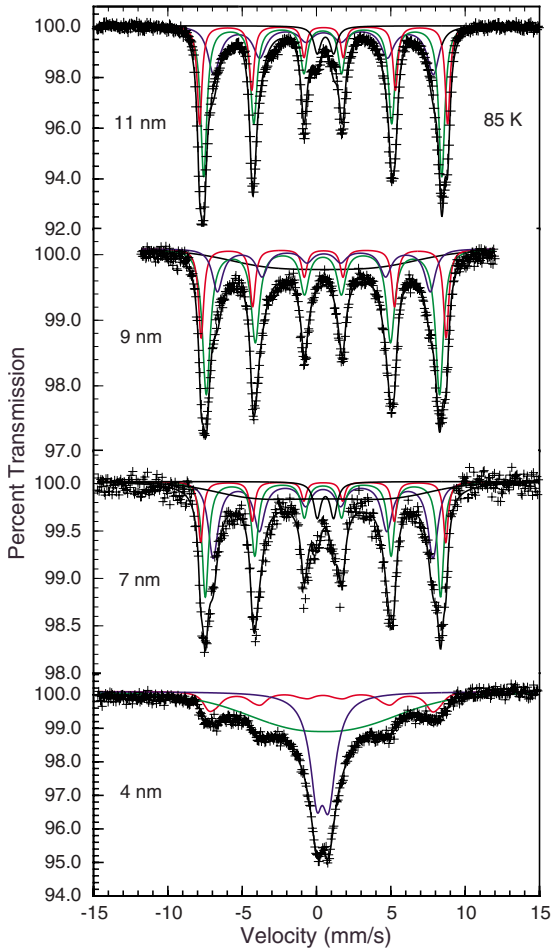

FIG. 2. (Color online) The 85 K Mössbauer spectra of the iron oxide nanoparticles with the indicated diameters.

material at room temperature that is blocked at 4.2 K.

The definition of a blocking temperature for superparamagnetic particles is always difficult and different authors use different definitions. For the purpose of giving at least an order of magnitude of the blocking temperatures in the present Mössbauer study, the blocking temperature is herein defined as the temperature at which the resolved doublet represents ~50% of the Mössbauer spectral absorption area. The blocking temperatures are thus 120(10), 225(20), 230(20), and >295 K for the 4, 7, 9, and 11 nm particles, respectively.

Qualitatively, the observed line shape profiles in Figs. 1–5 are similar to those observed in many of the earlier Mössbauer studies[7,8] of polydispersed iron oxide nanoparticles. This similarity was at first surprising as a broad distribution of blocking temperatures and hence of hyperfine fields was not expected for highly monodispersed iron oxide nanoparticles. The error of ±0.2 nm in the 9 nm diameter particles corresponds to an expected 7 K distribution in the blocking temperatures. Because of the monodispersed nature, fits with a distribution of hyperfine fields, as used in earlier studies,[6,8] could not be justified. In contrast, fits with a relaxation profile resulting from fluctuations of the nanoparticle magnetic moments are easily justified. Hence, the Mössbauer spectra shown in Figs. 1–5 have been fitted within the stochastic relaxation model developed by Dattagupta and Blume.[17–19] In this model the system randomly adopts different stochastic states and the Hamiltonian matrix describing each of these states switches from the initial stochastic state to the final stochastic state with a probability that is independent of the initial state. This assumption simplifies the calculations and is valid in many cases such as for the thermal relaxation of the magnetic hyperfine field in superparamagnetic materials. In the fits shown in Figs. 1–5, the magnetic field is assumed to relax[19] between all six of the $\pm x$, $\pm y$, and $\pm z$ directions in space, an assumption that is sufficient to model the relaxation of the magnetic field caused by the thermal activation of the magnetic moment in each nanoparticle. It should be noted, as expected for spherical nanoparticles, that the spectra could not satisfactorily be modeled with the assumption that the magnetic field is relaxing anisotropically along the $\pm z$ directions in space. Because the Mössbauer spectra at 295 K show the presence of a quadrupole interaction, we have introduced a quadrupole interaction in the Hamiltonian used for the fits of the spectra that clearly show the presence of a doublet. At 4.2 K no sextet quadrupole shift is observed in the spectra, most likely because of the random orientation of the hyperfine field relative to the electric field gradient

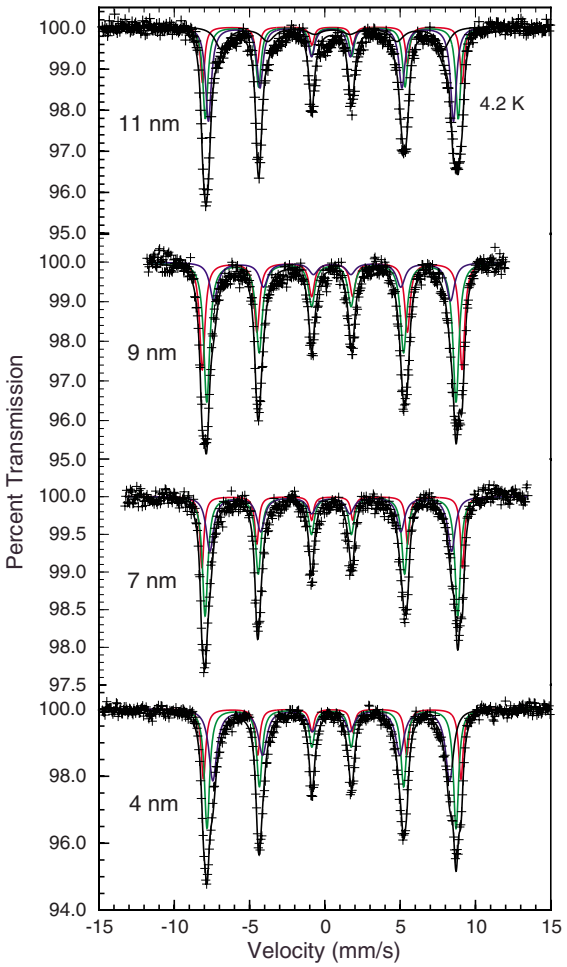

FIG. 3. (Color online) The 4.2 K Mössbauer spectra of the iron oxide nanoparticles with the indicated diameters.

principal axes. Hence, a zero quadrupole interaction was introduced into the Hamiltonian for the spectra showing magnetic order. Further, the broadening of the spectra at intermediate temperatures completely dominates any effect of the quadrupole interaction such that it cannot be detected.

The 4.2 K spectra do not show the complexity of the 4.2 K spectrum of bulk magnetite.[20] However, because nanoparticles of Fe_3O_4 do not exhibit[21] the Verwey transition, their Mössbauer spectra are virtually identical to those of γ-Fe_2O_3. Hence it is difficult to determine whether or not magnetite is present[5] in the nanoparticles. At 4.2 K the spectra have been fitted with three relaxation profiles with hyperfine fields of ~50 T, zero quadrupole interactions, slightly different isomer shifts, and slow relaxation frequencies of a few MHz. The two most intense sextets are characteristic of the tetrahedral and octahedral sites of bulk maghemite[8] with slightly different isomer shifts and hyperfine fields, differences that account for the slight asymmetry in the outer lines of the 4.2 K spectra. As the temperature increases above 4.2 K, a broad relaxation profile with an intermediate relaxation frequency of ~10–20 MHz appears and at the highest temperature, a relaxation doublet with a high frequency of 500–800 MHz dominates the spectrum. The relaxation frequency associated with the narrow doublet has been determined by finding the lowest frequency that is consistent with the narrow central doublet, see, for instance, Fig. 4(a). These fits revealed that an additional broad component with a smaller relaxation frequency was superimposed on the narrow doublet. In fitting the broad relaxation profile, the hyperfine field and the relaxation frequency cannot be simultaneously fitted because of the large negative correlation between these two parameters. Hence, the hyperfine field was constrained to a value that exhibits weak temperature dependence, decreasing from ~51.5 to ~42 T between 4.2 and 295 K. As indicated by the solid lines in Figs. 1–5 the fits are good to excellent and, as a consequence, they provide confidence in the adequacy of the relaxation model used herein. Similar results and fits, not shown, were obtained for the temperature dependence of the Mössbauer spectra of the 7 and 11 nm particles.

Because it is not possible to discuss the temperature dependence of all the hyperfine parameters fitted in Figs. 1–5, only the temperature dependence of the weighted average isomer shift, hyperfine field, and relaxation rate is shown in Fig. 6 for the 4 and 9 nm particles. The 4.2 K weighted average isomer shift of 0.45(1) mm/s agrees very well with the previously reported values.[8] This isomer shift is typical of iron(III) oxide and there is no indication of the presence of any iron(II) component in the Mössbauer spectra—hence the particles contain less than 5%–10% of magnetite. The temperature dependence of the isomer shift, see Fig. 6, is similar for all the nanoparticles, is typical[22] of the second-order Doppler shift, and yields Mössbauer temperatures, Θ_M, of 635(45), 713(81), 714(50), and 647(67) K for the 4, 7, 9, and 11 nm particles, respectively. These Θ_M values are characteristic of iron(III) oxide materials.

The logarithm of the relaxation frequency versus the inverse temperature between 4.2 and 295 K for the 4 and 9 nm iron oxide nanoparticles is shown in Fig. 7. Three relaxation regimes, between 315 and ~125 K a thermally activated superparamagnetic behavior, between ~125 and 30 K a superparamagnetic behavior modified by interparticle interactions, and between 30 and 4.2 K a spin-glass-like behavior, are clearly visible for the 9 nm particles, an observation that agrees with the three regimes observed in the μ-spin relaxation studies, see Sec. IV. Similar plots have been obtained for the 7 and 11 nm nanoparticles, whereas only two relaxation regimes are observed for the 4 nm nanoparticles. The inset in Fig. 7 shows the logarithm of the relaxation frequency versus the inverse temperature between 30 and 295 K for the 4 and 9 nm nanoparticles. The activation energies in the different regimes are given in Table I. At 4.2 K the relaxation is very slow and the observed relaxation rate mimics the slight broadening of the absorption lines, a broadening that could result from a narrow distribution of hyperfine fields corresponding to the core and shell iron(III) ions. At high temperatures, typically above 125 K, a fast relaxation regime is observed in all the iron oxide nanoparticles. The activation energy of this regime increases from 148(4) to 1326(50) K with increasing particle diameter, as expected for a superparamagnetic material. In the intermediate-temperature range, an intermediate relaxation rate is observed with an activation energy of ~100 K in the 7, 9, and 11 nm iron oxide nanoparticles.

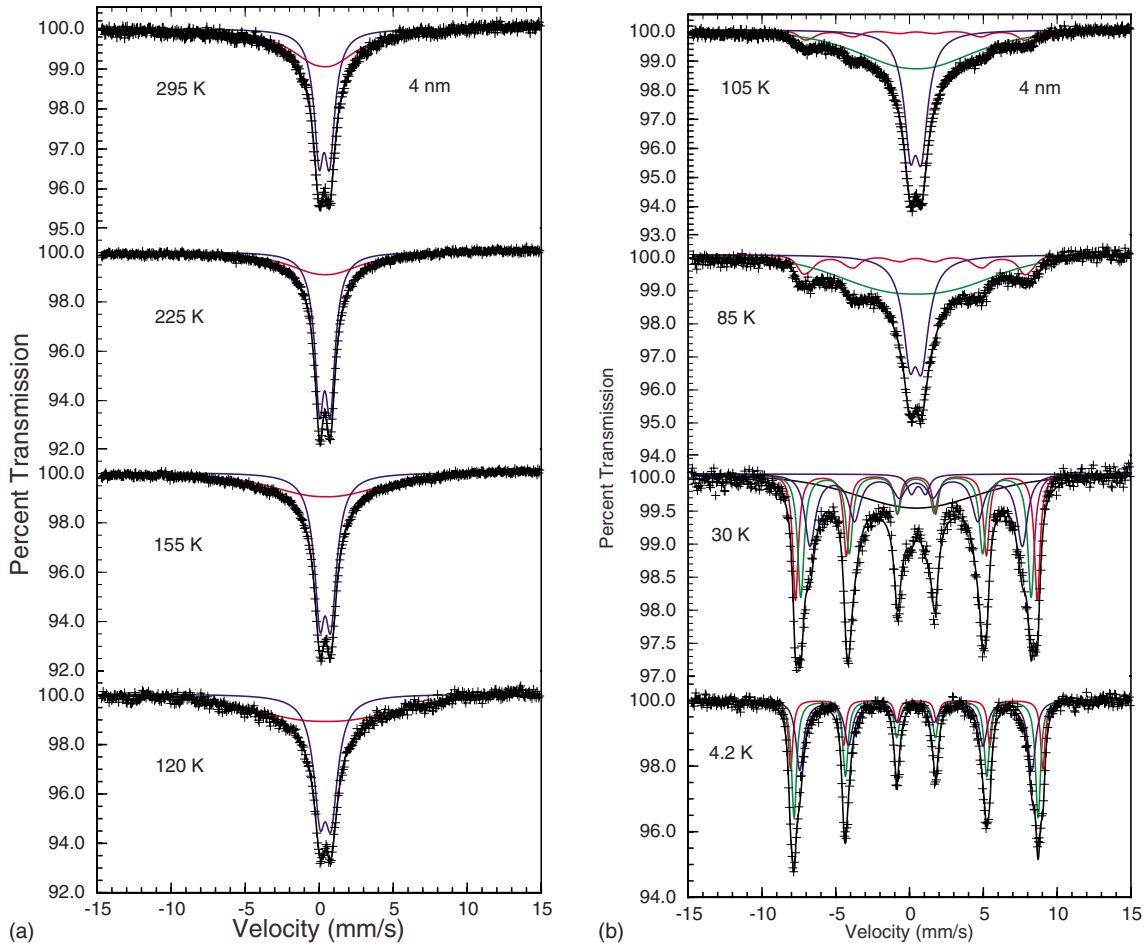

FIG. 4. (Color online) [(a) and (b)] The Mössbauer spectra of the 4 nm iron oxide nanoparticles obtained at the indicated temperatures.

The temperature dependence of the logarithm of the total absorption for the 4 and 9 nm iron oxide nanoparticles is shown in Fig. 6. Similar results have been obtained for the 7 and 11 nm particles and a fit of the results with the Debye model[22] for the Mössbauer spectral absorption area yields effective Debye temperatures, Θ_D, of 237(4), 262(17), 249(9), and 400(22) K for the 4, 7, 9, and 11 nm nanoparticles, respectively, values that are both smaller than the 440(30) K observed[23] for bulk γ-Fe_2O_3 and smaller than the 460(50) and 380(50) K values observed,[23] respectively, for uncoated and coated 12 nm γ-Fe_2O_3 nanoparticles. Indeed, it would be expected that the spectral absorption area will decrease faster with decreasing particle size, because of both possible vibrations[23] of the particles and surface effects. Furthermore, it is interesting to note that at 295 K the absorption area observed of the 4 nm particles is far lower than expected on the basis of the Debye fit, see Fig. 6; a similar but smaller discrepancy is observed at 295 K for the 7 nm particles. These small absorption areas are an indication, at least for the 4 and 7 nm particles, that the iron(III) recoil-free fraction has decreased substantially at 295 K as a result of the preponderance of iron(III) on the surface of the nanopar-

TABLE I. The magnetic relaxation activation energies and the corresponding magnetic anisotropy constants.

	Intermediate regime		High-temperature regime		
Diameter (nm)	Range (K)	Energy (K)	Range (K)	Energy (K)	K (10^4 J/m^3)
4.0(1)	30–295	148	30–295	148(4)	4.7(5)
7.0(2)	30–125	112	125–295	453(25)	3.5(5)
9.0(2)	30–120	112	120–295	540(23)	2.0(2)
11.0(2)	80–150	77	150–295	1326(50)	2.6(2)

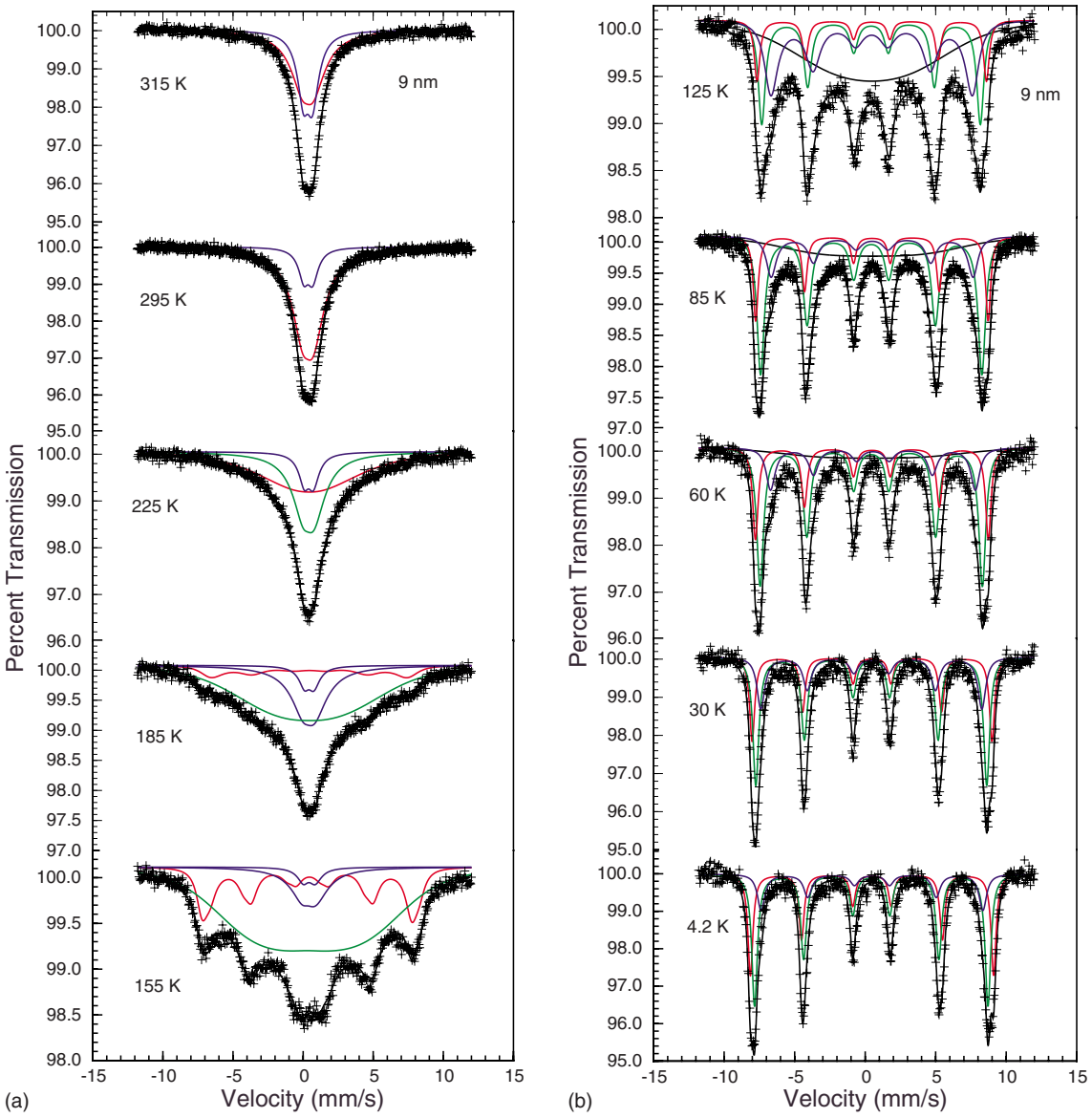

FIG. 5. (Color online) [(a) and (b)] The Mössbauer spectra of the 9 nm iron oxide nanoparticles obtained at the indicated temperatures.

ticles. The number of iron(III) ions on or near the surface may be estimated from the size of the particles and the unit cell volume of bulk γ-Fe_2O_3. If the "surface" is assumed to consist of one unit-cell layer, then this surface contains 970, 3700, 6400, and 10 000 iron(III) ions and thus 78%, 55%, 46%, and 38% of the iron(III) ions in the particle are contained within the surface of the 4, 7, 9, and 11 nm nanoparticles, respectively. If the surface is assumed to consist of two unit-cell layers, the corresponding values are 1100, 5500, 10 400, and 16 800 iron(III) ions and 85%, 82%, 73%, and 65%. Thus, under either assumption, it is clear that a substantial portion of the iron(III) ions can be considered to be surface ions—especially in the 4 nm particles. Thus it seems that the expected reduction in the recoil-free fraction at and near the surface of a nanoparticle results in the observed decrease in the spectral absorption area for the smaller particles at the higher temperatures.

IV. μ-SPIN RELAXATION RESULTS

For the μ-spin relaxation studies, spin-polarized muons have been implanted into the 9 nm iron oxide nanoparticles. The spins of the implanted muons rotate about any local field that is not parallel with their initial polarization[24] and thus any variation in the implantation sites or fields within the nanoparticles leads to a depolarization of the muon spin. The mean lifetime of the muon, t_μ, is 2.2 μs and the muon decays by emitting a positron preferentially in its spin direction. Therefore a muon-spin depolarization will be mirrored by a relaxation of the positron-signal asymmetry between detectors located on opposite sides of the sample along the initial muon-polarization direction.

Examples of the asymmetry measured at 2, 30, 90, and 250 K under a zero applied field for the 9 nm iron oxide nanoparticles are shown in Fig. 8. It should be noted that at

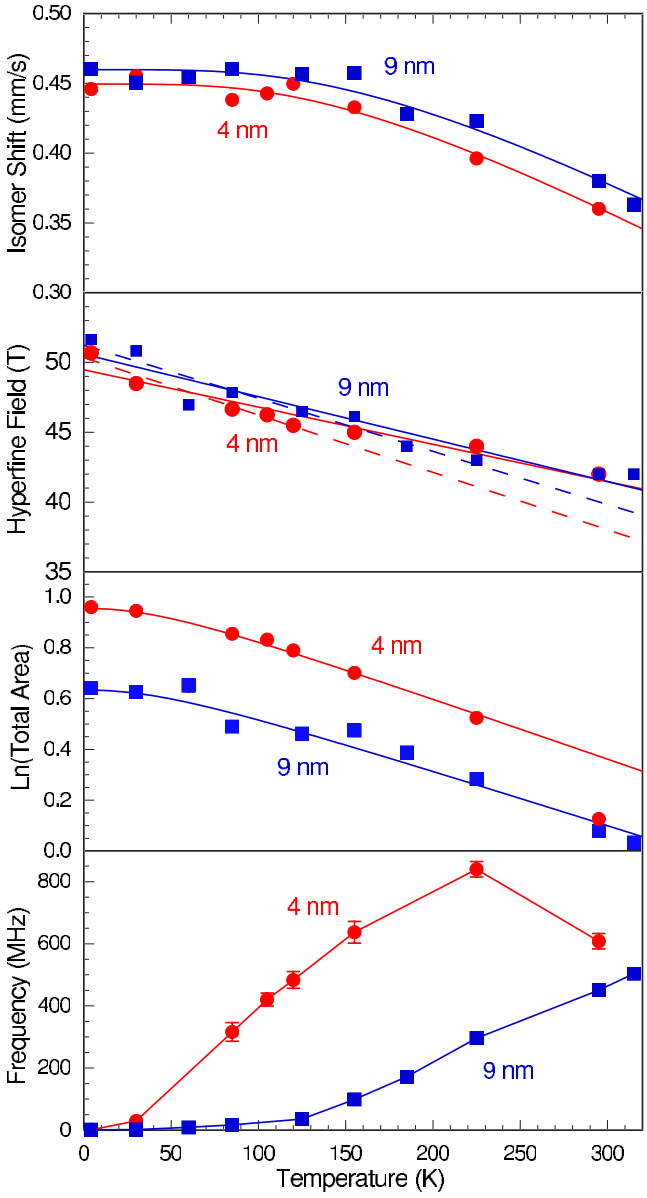

FIG. 6. (Color online) The temperature dependence of the weighted average isomer shift, hyperfine field, and relaxation rate, and the logarithm of the total absorption area for the 4 nm, red circles, and the 9 nm, blue squares, diameter particles. The dashed and solid straight lines in the temperature dependence of the hyperfine field are the results of fits with Eq. (7), below the blocking temperature and between 4.2 and 295 K, respectively. The reader should note that the 4 nm 295 K data point for the logarithm of the total absorption area is not included in the Debye model fit shown. The error bars for the isomer shifts, hyperfine fields, and the logarithm of the total areas are approximately the size of the data points. The error bars for the relaxation frequency are either shown or are approximately the size of the data points.

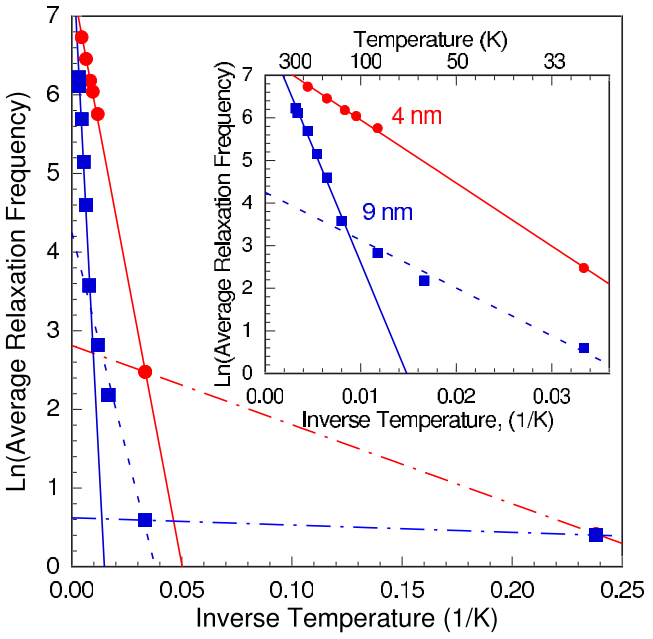

FIG. 7. (Color online) The logarithm of the weighted average relaxation frequency versus $1/T$ obtained for the 4 nm diameter, red circles, and 9 nm diameter, blue squares, iron oxide nanoparticles. Inset: the logarithm of the relaxation frequency versus $1/T$ for the 4 and 9 nm diameter iron oxide nanoparticles, obtained above 4.2 K. The solid, dashed, and dash-dotted lines are the linear least-square fits in the high-, intermediate-, and low-temperature regimes, respectively.

250 K, and from 125 to 315 K, the asymmetry decays to zero after ~1 μs, whereas below 125 K, it decays to a nonzero value, a value that increases to ~0.07 at 4 μs at 2 K. In the superparamagnetic regime, at and above 125 K, the muons in their various resting environments experience a distribution of local fields, fields that fluctuate with a relaxation time, τ. In this regime, the muon-depolarization function for a fluctuating magnetization in monodispersed nanoparticles[16] is given by

$$a_0 G_z(t) = a_0 \exp[-(\sigma t)^{0.5}], \tag{1}$$

where σ is the relaxation rate of the muon and a_0 represents the initial asymmetry parameter, which depends mainly on the instrument geometry and can be obtained by calibration procedures. In the present measurements a_0 was found to be ~0.25. The stretched exponential form of Eq. (1) is a consequence of averaging over different fluctuating local fields at different muon sites. In this model, the muon relaxation rate is proportional to the nanoparticle magnetic moment fluctuation time, τ, and to the square of the width of the field distribution. By assuming a Lorentzian field distribution with a half width at half maximum, ΔB, the muon relaxation rate at a temperature, T, can be expressed as

$$\sigma(T) = 4(\gamma_\mu \Delta B)^2 \tau(T), \tag{2}$$

where γ_μ is the muon gyromagnetic ratio, given by $\gamma_\mu/2\pi = 135.5$ MHz/T.

At and above 125 K, the asymmetry data have been successfully fitted with Eq. (1) confirming the excellent monodispersed nature of the 9 nm iron oxide nanoparticles. If a distribution of rates was present, the power law in the asymmetry function would significantly vary[25] from the observed value of 0.5. The fit of the asymmetry function, $a_0 G_z(t)$, at

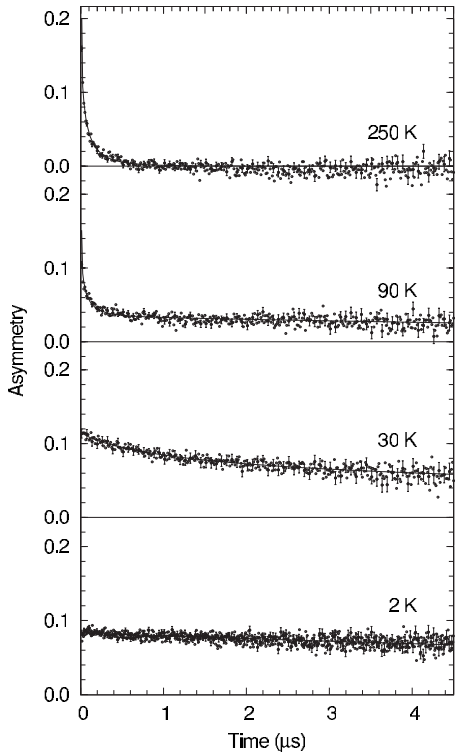

FIG. 8. The μ-spin relaxation asymmetry functions for the 9 nm diameter iron oxide nanoparticles obtained at the indicated temperatures. The solid lines are the results of the fits discussed in the text. The error bars are indicated on every fifth data point.

250 K with Eq. (1) is shown in Fig. 8 as the solid line, and the 125–315 K temperature dependence of the corresponding relaxation rate, σ, is shown in Fig. 9.

Below 125 K the local fields experienced by the muons become progressively more static with decreasing temperature. Thus below 125 K the ensemble of muons must be divided into two parts, the first part, a_1, experiences a relaxing field in a fashion similar to that observed above 125 K but with a reduced relaxation rate, σ, whereas the second part, a_2, experiences a broad distribution of static local fields. The observation of two components in the μ-spin relaxation signal, with respective weights, a_1 and a_2, reflects a volume segregation, with a volume fraction, a_1/a_0, still exhibiting a paramagnetic state and a fraction, a_2/a_0, exhibiting a static magnetic state. Because the sample is a powder, this latter volume fraction is itself represented by a two-component asymmetry function. Furthermore, because the sample is polycrystalline, the first subcomponent, with a relative weight of $2a_2/3$, should show oscillations, whereas the second subcomponent, with a relative weight of $a_2/3$, should show only an exponential decay if dynamic relaxation is still present.[26] This latter part represents muons having their initial polarization align along the local field. As is shown at 90, 30, and 2 K in Fig. 8, no oscillations are observed below 120 K, most likely because the muons experience a large local field and/or a broad distribution of the local fields. Hence, all the results obtained below 125 K have been fitted with the expression

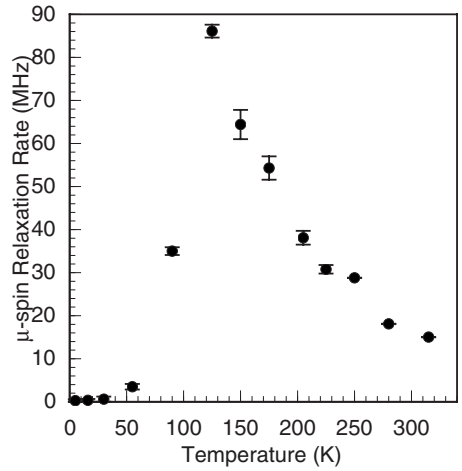

FIG. 9. The temperature dependence of the μ-spin relaxation rate, σ, obtained at zero field for the 9 nm diameter iron oxide nanoparticles.

$$a_0 G_z(t) = a_1 \exp[-(\sigma t)^{0.5}] + (a_2/3)\exp(-\lambda t), \qquad (3)$$

where the sum of a_1 and a_2 has been kept equal to the initial asymmetry, i.e., $a_0=0.25$, in order to take into account the constant total volume of the sample. Just below the 120 K transition λ is $\sim 0.07\ \mu s^{-1}$, a small value that reflects some residual fluctuations in the nearly static magnetic volume. The value of λ decreases gradually upon further cooling, a decrease that is an indication of an essentially static magnetic state at the lowest temperatures. All the fits obtained are excellent, and the resulting relaxation rate, σ, decreases with decreasing temperature, as is shown below 125 K in Fig. 9. The volume fraction of the sample, a_1, experiencing the superparamagnetic relaxation also decreases with decreasing temperature below 125 K, as is shown in Fig. 10. The temperature dependence of a_2 was fitted with the expression

$$a_2 = a_0[1 - (T/T_c)]^{\beta}, \qquad (4)$$

with $T_c=125$ K and $\beta=0.72$.

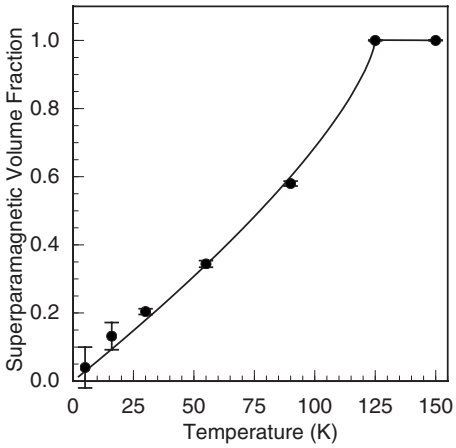

FIG. 10. The temperature dependence below 125 K of the volume fraction of the monodispersed particles experiencing superparamagnetic relaxation. The solid line is the result of the fit discussed in the text.

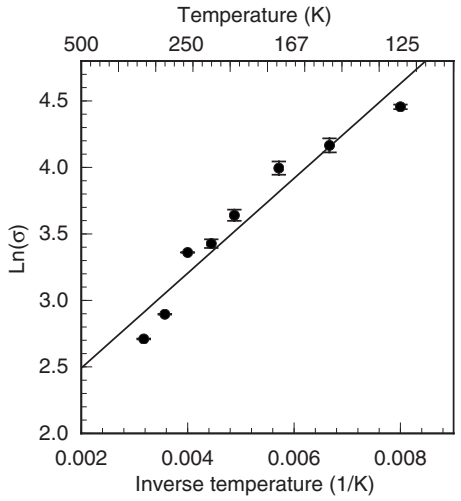

FIG. 11. The logarithm of the μ-spin relaxation rate, σ, obtained between 125 and 315 K versus $1/T$ for the 9 nm nanoparticles.

The temperature dependence of the muon relaxation rate, σ, see Fig. 9, is at a maximum at 125 K, corresponding to the blocking temperature as probed by the muons.[27] This maximum reflects the broad distribution of local fields created by the nanoparticles, nanoparticles that exhibit a broad distribution of relaxation rates, as is indicated by the Mössbauer spectra. In agreement with Eq. (2) above the blocking temperature, the observed reduction of σ reflects an increase in the fluctuation rate of the magnetic moment of the nanoparticles. Below the blocking temperature, the observed decrease in σ reflects a decrease of the field distribution at the muon site resulting from interparticle dipolar interactions, interactions which modify the superparamagnetic behavior.[7–9]

The temperature dependence of the relaxation rate at and above 125 K is shown in an Arrhenius plot in Fig. 11. The linear fit shown in Fig. 11 yields an intrinsic relaxation rate of 6(1) MHz and an activation energy, E_{act}, of 356(20) K. This activation energy and the 382 nm^3 volume of a 9 nm diameter nanoparticle yields an anisotropy constant, K, of $1.3(1)\times 10^4$ J/m^3.

At this point, it is worth noting that the exact stopping site of the muons is not known and it could be inside the particles, in the oleic acid surrounding the particles, or at this interface. However, the successful fits above 125 K with Eq. (1) indicate that the muons experience only one relaxation rate and thus experience similar environments in their different stopping sites. Furthermore, the absence of the oscillating component in Eq. (3) strongly suggests that the majority of the muons stop inside the nanoparticles, where they experience a large field.

V. DISCUSSION

From both the Mössbauer spectral and μ-spin relaxation measurements on monodispersed iron oxide nanoparticles, three magnetodynamic regimes have been identified between 4.2 and 315 K. The temperature range of each of these regimes depends on the particle diameter, as is indicated in Table I. The low-temperature regime is a spin-glass-like regime, the high-temperature regime is a thermally activated superparamagnetic regime, and the intermediate-temperature regime is a superparamagnetic regime modified by dipolar interparticle magnetic interactions. The existence of this intermediate regime is unexpected for monodispersed particles, but it is strongly supported by both the Mössbauer spectral and μ-spin relaxation results. The activation energies observed in the intermediate-temperature regime by Mössbauer spectroscopy *decrease* from 148 to 77 K with increasing diameter, see Table I. This small factor of 2 change indicates that the dynamic process taking place in the intermediate-temperature regime must be controlled by interparticle interactions rather than by the particle volume. Further more, these small activation energies, as compared with those observed in the high-temperature regime, see Table I, indicate that they are associated with the reversal of one or a few atomic spins at the surface of the particles rather than with the reversal of the magnetic moment of an entire particle. The intermediate-temperature regime is similar to the collective magnetic excitation regime described by Mørup and co-workers.[28–31] In contrast, in the high-temperature regime, the activation energies *increase* from 148 to 1326 K with increasing diameter, i.e., a factor of 10 increase. This large change indicates that the dynamic process occurring in the high-temperature regime must be controlled by the particle volume.

The blocking temperatures reported from the magnetic susceptibility,[3,5] Mössbauer spectral, and μ-spin relaxation measurements are given in Table II. Because the characteristic measuring times of these techniques are different, the blocking temperatures are different. The characteristic time, τ_m, of magnetic susceptibility, μ-spin relaxation, and Möss-

TABLE II. Blocking temperatures, T_B, and corresponding magnetic anisotropy constants, K.

Diameter (nm)	Magnetic susceptibility[a]		μ-spin relaxation		Mössbauer spectroscopy	
	T_B (K)	K (10^4 J/m^3)	T_B (K)	K (10^4 J/m^3)	T_B (K)	K (10^4 J/m^3)
4.0(1)	25	20			120	19.5
7.0(2)	40	12.5			225	6.9
9.0(2)	110	7.5	125	4.2; 1.3(1)[b]	230	3.3
11.0(2)	190	4.0			295	2.3

[a]Values obtained from Ref. 4.
[b]Value obtained from the temperature dependence of the relaxation rate.

bauer spectral measurements are of the order of 10, $\sim 10^{-6}$, and 5×10^{-9} s, respectively. As a result, in the magnetic susceptibility measurements, the magnetic moment of the nanoparticles is blocked at temperatures lower than those observed in the μ-spin relaxation and the iron-57 Mössbauer spectral measurements.

The magnetic anisotropy constant, K, of the nanoparticles can be obtained from the blocking temperatures observed by the three different techniques from

$$KV = \ln(\tau_m/\tau_0) k_B T_B, \tag{5}$$

where τ_m is the characteristic time of the measurements, τ_0 is the intrinsic fluctuation time of the nanoparticles, k_B is Boltzmann's constant, T_B is the blocking temperature, and V is the particle volume. The anisotropy constants determined from Eq. (5) by using $\tau_0 = 10^{-10}$ s, a typical value,[6,30,31] and the τ_m values given above, are given in Table II. All these values are in fair agreement and are larger than the magnetocrystalline anisotropy of 0.47×10^4 J/m^3 observed in bulk γ-Fe_2O_3. The difference between the bulk and the observed magnetic anisotropy constants results from a combination of surface magnetic anisotropy and interparticle interactions of the nanoparticles. Indeed, interacting γ-Fe_2O_3 nanoparticles synthesized[24] by a coprecipitation technique have an anisotropy constant of 0.35×10^4 J/m^3, i.e., they approach the bulk value. In contrast, noninteracting particles[32–34] have values of the order of 10×10^4 J/m^3. In the following discussion we try to separate the surface and interparticle influences and to determine whether or not there is a volume dependence of the magnetic anisotropy constant for the monodispersed iron oxide nanoparticles understudy.

The magnetic anisotropy constants of the 4, 7, 9, and 11 nm diameter nanoparticles have also been obtained from the activation energy of the thermally activated superparamagnetic behavior observed in the Mössbauer spectra and are given in Table I. The values obtained for the 9 and 11 nm nanoparticles are in excellent agreement with the value of $2.1(3) \times 10^4$ J/m^3 obtained[35] for polydispersed spherical maghemite nanoparticles with a mean diameter of 10.3(5) nm. Further more, an anisotropy constant of $1.3(1) \times 10^4$ J/m^3 has been obtained from the activation energy determined from the μ-spin relaxation rate above 125 K for the 9 nm diameter nanoparticles. This value is significantly different from the $2.0(2) \times 10^4$ J/m^3 value obtained by Mössbauer spectroscopy, a difference that may be related to the different types of relaxations observed by the two techniques, i.e., the relaxation of the local magnetic field at the muon resting site and the relaxation of the magnetic hyperfine field at the iron-57 nucleus. All of the magnetic anisotropy constants obtained from activation energies, see Table I, are smaller than those obtained from the blocking temperatures, see Table II. We believe that, as previously observed[30] for hematite nanoparticles, the magnetic anisotropy constants obtained from the activation energies in the high-temperature thermally activated superparamagnetic regime are less dependent on the interparticle interactions and more dependent on the volume.

Because of differing results reported[4,5] earlier for the diameter dependence of the magnetic anisotropy constants, the magnetic anisotropy constants reported earlier and in Table I have been plotted as a function of particle diameter in Fig. 12; the solid lines in this figure are the result of linear least-squares fits. In this figure, the 5 nm, 20×10^4 J/m^3 value reported in Ref. 4 has been omitted. We conclude that both sets of anisotropy constants indicate that the monodispersed iron oxide nanoparticles exhibit a decrease in magnetic anisotropy with increasing diameter. Of course, as mentioned above, the magnetic anisotropy constants obtained from Mössbauer spectroscopy, the circles in Fig. 12, are smaller than those obtained from magnetic susceptibility measurements, the blue squares in Fig. 12. However, there is a virtually diameter independent difference between the two sets of values, a difference that could result from the contribution of interparticle interactions to the magnetic anisotropy.

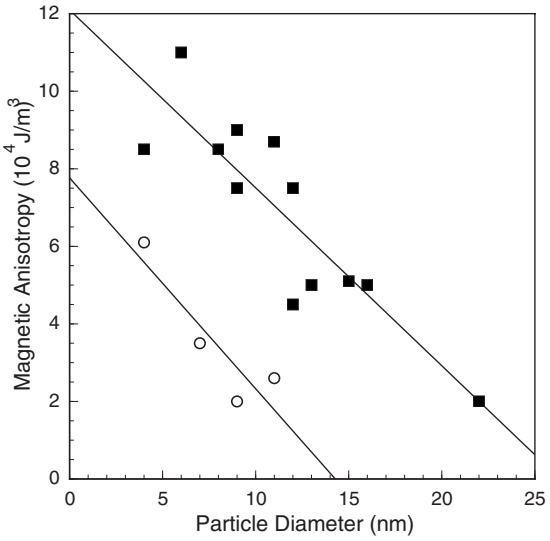

FIG. 12. The diameter dependence of the magnetic anisotropy constant. The squares are values obtained from Refs. 4 and 5 and the circles are the values given in Table I. The solid lines are the result of a linear least-squares fit.

In an attempt to further investigate the surface contribution, the magnetic anisotropy constants of the monodispersed iron oxide nanoparticles obtained from Refs. 4 and 5, and from the present Mössbauer spectral studies have been plotted as a function of the percentage of iron(III) ions present in a one unit-cell shell at the surface of the nanoparticles, see Fig. 13. The solid lines are the results of fits with the linear equation

$$K = K_b(1-p) + K_s p, \tag{6}$$

where p is the percentage iron(III) on the surface, K_b is the bulk anisotropy constant of γ-Fe_2O_3 and is constrained to 0.47, and K_s is the magnetic anisotropy for the surface shell; K, K_b, and K_s have units of 10^4 J/m^3. If a surface shell of 0.35 nm thickness[6] is used, a similar linear correlation is observed. The fits are reasonably good and support the idea that there is a substantial contribution of the surface to the magnetic anisotropy of the nanoparticles understudy.

The temperature dependence of the weighted average hyperfine field is similar for the 4 and 9 nm particles and is

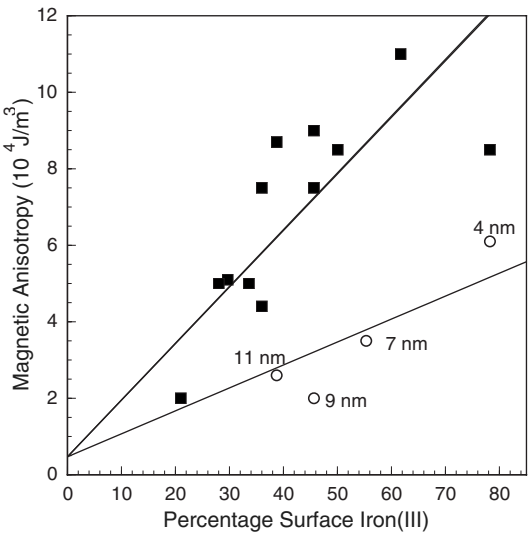

FIG. 13. The magnetic anisotropy constant as a function of the percentage of iron(III) ions present in a one unit-cell shell on the surface of the iron oxide nanoparticles. The squares are values obtained from Refs. 4 and 5 and the circles are the values given in Table I. The solid lines are the result of a fit with Eq. (6).

shown in Fig. 6. The decrease with increasing temperature is larger than that observed in bulk γ-Fe_2O_3. This larger decrease has been reported earlier and discussed in terms of either spin canting[8] at the surface of the nanoparticles or collective magnetic excitations[6,30,31,35–37] in the grains. In the latter model, the temperature dependence of the weighted average hyperfine field below the blocking temperature of the nanoparticles follows the expression

$$B_{\mathrm{hf}}(T) = B_0\{1 - [k_{\mathrm{B}}T/(2KV + 3k_{\mathrm{B}}T^*)]\}, \qquad (7)$$

where k_{B} is the Boltzmann constant, K is the magnetic anisotropy constant of a nanoparticle, V is the volume of the particle, and T^* is a temperature characteristic of the exchange anisotropy between particles, i.e., a measure of the interparticle interactions. The dashed and solid lines fitting the hyperfine field in Fig. 6 are the results of fits with Eq. (7), below the blocking temperature and between 4.2 and 295 K, respectively. By using the known volume of the 9 nm particles and the anisotropy constants of 1.3×10^4 and 2.0×10^4 J/m^3, obtained from the μ-spin relaxation and Mössbauer spectral studies, respectively, T^* values of 212 and 89 K are obtained. These temperatures are smaller than the 550 K value observed for 5.5 nm α-iron nanoparticles, for which the magnetic interactions were described as strong, and also smaller than the 320 K estimated[35] dipolar contribution to the magnetic anisotropy energy for interacting 7–10 nm Fe_3O_4 nanoparticles. Hence, as has been pointed[5] out earlier, the iron oxide nanoparticles understudy herein exhibit some interparticle magnetic interactions.

The dipolar field created by one 9 nm particle of maghemite at a distance of 12 nm is estimated to be ~0.03 T and, hence, the magnetic energy associated with the orientation of the magnetic moment of another 9 nm particle in this field is $\sim5\times10^{-21}$ J or a temperature of ~300 K, a value that is comparable to those quoted above.

The relaxation frequencies obtained by Mössbauer spectroscopy and μ-spin relaxation are different and are not directly comparable. In Mössbauer spectroscopy, the relaxation frequency is the frequency of the hyperfine field probed by the iron-57 nuclei, whereas in μ-spin relaxation, it is the relaxation frequency of the local field probed by the muon at its decay site. The relaxation frequencies measured by Mössbauer spectroscopy are larger than those measured by muon-spin relaxation, a difference that is in agreement with the characteristic times of the two techniques.

The observed broadening of the Mössbauer spectra was rather unexpected on the basis of the monodispersed nature of the nanoparticles, a property that should lead to one well-defined relaxation rate for the hyperfine field above and below the blocking temperature if the interparticle interactions are negligible. In contrast, a distribution of relaxation rates, which has been modeled with several relaxation rates in the present fits, is observed. This distribution of relaxation rates results from the differing interparticle interactions, interactions that result from the various different three-dimensional packing arrangements, faults in the aggregated nanoparticles, different near-neighbor environments of the different nanoparticles, and a small but nonzero distribution in the diameters of the nanoparticles.

On the basis of both the Mössbauer spectral and μ-spin relaxation results, we can propose a description of the magnetic state of the nanoparticle samples at intermediate and low temperatures. As the temperature decreases below 125 K, the interparticle magnetic interactions for some of the particles are strong enough to produce collective alignment of the magnetic moment in a few neighboring nanoparticles, i.e., to form a small cluster that would be rather similar to a domain in a ferromagnetic material. Upon further cooling, magnetic "percolation" expands and, below ~30 K, extends the collective alignment throughout the entire material. Thus, in the intermediate-temperature regime, the sample would consist of an ensemble of clusters with frozen spins, observed as the sextets in the Mössbauer spectra and as the fraction a_2 in the μ-spin relaxation results, immerged in a sea of unfrozen spins, observed as the doublet in the Mössbauer spectra and as the fraction a_1 in the μ-spin relaxation results.

VI. CONCLUSIONS

The goals of this study, as given in the Introduction, have been achieved. The μ-spin relaxation measurements clearly reveal the monodispersed nature of the nanoparticles, a nature that is confirmed by the experimentally unchecked model proposed by Lord.[16]

Both the μ-spin relaxation and Mössbauer spectral measurements have identified three regimes of magnetodynamic behavior between 4.2 and 300 K. The high-temperature regime is a thermally activated superparamagnetic regime with an activation energy increasing with increasing particle diameter. The low-temperature regime is a spin-glass-like regime. The existence of the intermediate regime in the magnetodynamics of monodispersed nanoparticles is unexpected

but its presence is well supported by both the μ-spin relaxation and Mössbauer spectral results. A qualitative description of the freezing of the spins in this regime has been proposed.

The Mössbauer spectra are not fully sensitive to the monodispersed nature of the particles because of substantial particle interactions, interactions that occur in spite of the oleic acid coating. Because fits with hyperfine field distributions commonly used to fit the Mössbauer spectra of polydispersed nanoparticles were not justified, the Mössbauer spectra of the monodispersed particles have been successfully fitted with a relaxation model that is consistent with the nearly spherical shape of the particles.

ACKNOWLEDGMENTS

The authors acknowledge with thanks the financial support of the Fonds National de la Recherche Scientifique, Belgium, through Grants No. 9.456595 and 1.5.064.05 and the Ministère de la Région Wallonne for Grant No. RW/115012. T.H. acknowledges the financial support of the Korean Ministry of Science and Technology through the National Creative Research Initiative Program of the Korea Science and Engineering Foundation. The μ-spin relaxation measurements were performed at the Swiss Muon Source of the Paul Scherrer Institute.

*Present address: Institut für Festkörperforschung, Forschungszentrum Jülich, Jülich GmbH, D-52425 Jülich, Germany.
†fgrandjean@ulg.ac.be
‡thyeon@snu.ac.kr
§alex.amato@psi.ch
‖glong@umr.edu

[1] G. Schmid, *Nanoparticles: From Theory to Application* (Wiley-VCH, Weinheim, 2004); K. J. Klabunde, *Nanoscale Materials in Chemistry* (Wiley-Interscience, New York, 2001); A. P. Alivisatos, Science **271**, 933 (1996); M. P. Pileni, Nat. Mater. **2**, 145 (2003).
[2] S. Sun, C. B. Murray, D. Weller, L. Folks, and A. Moser, Science **287**, 1989 (2000); D. E. Speliotis, J. Magn. Magn. Mater. **193**, 29 (1999).
[3] T. Hyeon, S. Seong Lee, J. Park, Y. Chung, and H. Bin Na, J. Am. Chem. Soc. **123**, 19798 (2001).
[4] J. Park, K. An, Y. Hwang, J. G. Park, H. J. Noh, J. Y. Kim, J. H. Park, N. M. Hwang, and T. Hyeon, Nat. Mater. **3**, 891 (2004).
[5] J. Park, E. Lee, N. M. Hwang, M. Kang, S. C. Kim, Y. Hwang, J. G. Park, H. J. Noh, J. Y. Kim, J. H. Park, and T. Hyeon, Angew. Chem., Int. Ed. **44**, 2872 (2005).
[6] E. Tronc, Nuovo Cimento Soc. Ital. Fis., D **18D**, 163 (1996); E. Tronc *et al.*, J. Magn. Magn. Mater. **221**, 63 (2000); J. L. Dormann, D. Fiorani, and E. Tronc, in *Advances in Chemical Physics*, edited by I. Prigogine and S. A. Rice (Wiley, New York, 1997), Vol. 98, p. 283.
[7] S. Mørup, F. Bødker, P. V. Hendriksen, and S. Linderoth, Phys. Rev. B **52**, 287 (1995).
[8] Ö. Helgason, H. K. Rasmussen, and S. Mørup, J. Magn. Magn. Mater. **302**, 413 (2006).
[9] L. Theil Kuhn, K. Lefmann, C. R. H. Bahl, S. Nyborg Ancona, P. A. Lindgård, C. Frandsen, D. E. Madsen, and S. Mørup, Phys. Rev. B **74**, 184406 (2006).
[10] T. Jonsson, J. Mattsson, C. Djurberg, F. A. Khan, P. Nordblad, and P. Svedlindh, Phys. Rev. Lett. **75**, 4138 (1995).
[11] T. Jonsson, P. Nordblad, and P. Svedlindh, Phys. Rev. B **57**, 497 (1998).
[12] C. Djurberg, P. Svedlindh, P. Nordblad, M. F. Hansen, F. Bødker, and S. Mørup, Phys. Rev. Lett. **79**, 5154 (1997).
[13] J. L. Dormann, L. Spinu, E. Tronc, J. P. Jolivet, F. Lucari, F. D'Orazio, and D. Fiorani, J. Magn. Magn. Mater. **187**, L139 (1998).
[14] D. Fiorani *et al.*, J. Magn. Magn. Mater. **196**, 143 (1999).
[15] P. Jönsson, T. Jonsson, J. L. Garcia-Palacios, and P. Svedlindh, J. Magn. Magn. Mater. **222**, 219 (2000).
[16] J. S. Lord, J. Phys.: Conf. Ser. **17**, 81 (2005).
[17] M. Blume, Phys. Rev. **174**, 351 (1968).
[18] S. Dattagupta and M. Blume, Phys. Rev. B **10**, 4540 (1974).
[19] R. P. Hermann, V. Keppens, P. Bonville, G. S. Nolas, F. Grandjean, G. J. Long, H. M. Christen, B. C. Chakoumakos, B. C. Sales, and D. Mandrus, Phys. Rev. Lett. **97**, 017401 (2006).
[20] R. E. Vandenberghe and E. De Grave, in *Mössbauer Spectroscopy Applied to Inorganic Chemistry*, edited by G. J. Long and F. Grandjean (Plenum, New York, 1989), Vol. 3, p. 59.
[21] A. D. Arelaro, A. L. Brandl, E. Lima, Jr., L. F. Gamarra, G. E. S. Brito, W. M. Pontuschko, and G. F. Goya, J. Appl. Phys. **97**, 10J316 (2005).
[22] G. K. Shenoy, F. E. Wagner, and G. M. Kalvius, in *Mössbauer Isomer Shifts*, edited by G. K. Shenoy and F. E. Wagner (North-Holland, Amsterdam, 1978), p. 49.
[23] S. Mørup, C. A. Oxborrow, P. V. Hendriksen, M. S. Pedersen, M. Hanson, and C. Johansson, J. Magn. Magn. Mater. **140-144**, 409 (1995).
[24] S. F. J. Cox, J. Phys. C **20**, 3187 (1987).
[25] I. A. Campbell, A. Amato, F. N. Gygax, D. Herlach, A. Schenck, R. Cywinski, and S. H. Kilcoyne, Phys. Rev. Lett. **72**, 1291 (1994).
[26] A. Schenck, *Muon Spin Rotation Spectroscopy* (Adam Hilger, Bristol 1985).
[27] T. J. Jackson *et al.*, J. Phys.: Condens. Matter **12**, 1399 (2000).
[28] F. Bødker, M. F. Hansen, C. B. Koch, K. Lefmann, and S. Mørup, Phys. Rev. B **61**, 6826 (2000).
[29] M. F. Hansen, C. B. Koch, and S. Mørup, Phys. Rev. B **62**, 1124 (2000).
[30] F. Bødker and S. Mørup, Europhys. Lett. **52**, 217 (2000).
[31] S. Mørup and C. W. Ostenfeld, Hyperfine Interact. **136**, 125 (2001).
[32] S. Linderoth, P. V. Hendriksen, F. Bødker, S. Wells, K. Davies, S. W. Charles, and S. Mørup, J. Appl. Phys. **75**, 6583 (1994).
[33] J.-R. Jeong, S.-C. Shin, S.-J. Lu, and J.-D. Kim, J. Magn. Magn. Mater. **286**, 5 (2005).
[34] D. Fiorani, A. M. Testa, F. Lucari, F. D'Orazio, and H. Romero, Physica B **320**, 122 (2002).
[35] D. Predoi, V. Kuncser, and G. Filoti, Rom. Rep. Phys. **56**, 373 (2004).
[36] S. Mørup, J. Magn. Magn. Mater. **37**, 39 (1983).
[37] Q. A. Pankhurst, D. H. Ucko, L. Fernandez Barquin, and R. Garcia Calderon, J. Magn. Magn. Mater. **266**, 131 (2003).